CHEMISTRY
AN ASIAN JOURNAL

DOI: 10.1002/asia.200700235

Bonding Analysis of N-Heterocyclic Carbene Tautomers and Phosphine Ligands in Transition-Metal Complexes: A Theoretical Study**

Ralf Tonner, Greta Heydenrych, and Gernot Frenking*[a]

Abstract: DFT calculations at the BP86/TZ2P level were carried out to analyze quantitatively the metal–ligand bonding in transition-metal complexes that contain imidazole (IMID), imidazol-2-ylidene (nNHC), or imidazol-4-ylidene (aNHC). The calculated complexes are $[Cl_4TM(L)]$ (TM = Ti, Zr, Hf), $[(CO)_5TM(L)]$ (TM = Cr, Mo, W), $[(CO)_4TM(L)]$ (TM = Fe, Ru, Os), and [ClTM(L)] (TM = Cu, Ag, Au). The relative energies of the free ligands increase in the order IMID < nNHC < aNHC. The energy levels of the carbon σ lone-pair orbitals suggest the trend aNHC > nNHC > IMID for the donor strength, which is in agreement with the progression of the metal–ligand bond-dissociation energy (BDE) for the three ligands for all metals of Groups 4, 6, 8, and 10. The electrostatic attraction can also be decisive in determining trends in ligand–metal bond strength. The comparison of the results of energy decomposition analysis for the Group 6 complexes $[(CO)_5TM(L)]$ (L = nNHC, aNHC, IMID) with phosphine complexes ($L = PMe_3$ and PCl_3) shows that the phosphine ligands are weaker σ donors and better π acceptors than the NHC tautomers nNHC, aNHC, and IMID.

Keywords: carbenes · bonding analysis · density functional calculations · N-heterocyclic carbenes · phosphine complexes

Introduction

The significance of N-heterocyclic carbenes (NHCs) has burgeoned apace over the last few years. The first transition-metal complexes with NHC ligands had already been synthesized in 1968 by Öfele[1] and by Wanzlick and Schönherr.[2] Great impact on research in the field was made by the isolation of the first free NHC by Arduengo et al. in 1991.[3] The revitalized experimental work showed that NHCs are versatile ligands in transition-metal chemistry.[4] Intensive investigative efforts in the synthesis[5] and catalytic applications, such as olefin metathesis,[6] carbon–carbon coupling,[7] hydrogenation,[8] and hydrosilylation,[9] of NHC complexes soon followed.

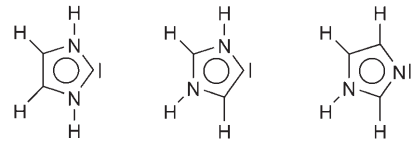

Scheme 1. The imidazole tautomers nNHC, aNHC, and IMID.

NHC ligands most commonly coordinate to metals in the C2 position (Scheme 1, left), and until recently, only complexes that carry "normal" NHC ligands (nNHCs) were known. The first C4/C5-coordinated NHC complex, the so-called "abnormal" carbene complex, was synthesized by Crabtree and co-workers[10] by the addition of variously substituted 2-pyridylimidazolium salts to $[IrH_5(PPh_3)]$. No rearrangement to the C2-bonded isomer occurred, even under heating. Since then, a number of other complexes with "abnormal" carbene ligands (aNHCs; Scheme 1, center) have been synthesized by the same group[11] and by others.[12] Specifically, it was found that two properties of the 2-pyridylimidazolium salt determines whether it binds normally (C2) or abnormally (C4/C5). First, the shorter the linker (hence, the smaller the bite angle), the more the C4/C5 carbene complex is formed, except when these positions are blocked. The product ratio is also shifted in favor of the C4/C5 car-

[a] R. Tonner, Dr. G. Heydenrych, Prof. Dr. G. Frenking
Fachbereich Chemie
Philipps-Universität Marburg
Hans-Meerwein-Strasse, D-35032 Marburg (Germany)
Fax: (+49) 6421-282-5566
E-mail: frenking@chemie.uni-marburg.de

[**] Theoretical Studies of Organometallic Compounds, Part 57. Part 56: A. Krapp, K. K. Pandey, G. Frenking, *J. Am. Chem. Soc.* **2007**, *129*, 7596.

Supporting information for this article is available on the WWW under http://www.chemasianj.org or from the author.

bene complexes with increasing size of the so-called wingtip groups R.[11b] Nonchelating examples of aNHCs have also been isolated,[11d] but they were found to be less stable. It was later discovered that the choice of counterion to the carbene ligand plays a critical role in determining whether the carbene coordinates normally or abnormally.[11a,c] Interestingly, the C4/C5 carbenes are expected to be better electron donors than their C2 counterparts, even though they were suggested to be more weakly bonded to the metal.[13] DFT calculations showed that free and complexed abnormal carbenes are higher in energy than normal carbenes.[14] The chemistry of abnormal carbenes was recently reviewed by Arnold and Pearson.[15]

The nNHC (imidazol-2-ylidene) and aNHC (imidazol-4-ylidene) carbenes are tautomeric forms of the most stable isomer imidazole (IMID; Scheme 1, right). As the imidazole ring is a moiety of histidine, in which it plays an important role in a variety of biologically important systems,[16] it has been studied extensively both as a free species and as a ligand in transition-metal complexes. The preferential C versus N binding in imidazole complexes was studied by Sini, Eisenstein, and Crabtree (SEC).[14a] They found that an important factor in deciding the ratio of N- to C2-coordinated groups in transition-metal complexes lies in the ligand *trans* to the carbene position. High-*trans*-effect ligands generally favor the *N*-imidazole, probably because transition-metal–N bonds tend to be longer than transition-metal–C bonds. However, in moving down the periodic table, the balance is shifted towards the carbene form, probably because the longer bonds overall tend to cancel the *trans* effect.[14a] Protonation reactions of aNHC, nNHC, and IMID were studied theoretically by Magill and Yates.[14b]

As NHCs have been termed the most important ancillary ligands after cyclopentadienyls and the ubiquitous phosphines,[13] much effort has been made to understand their electronic structure and binding modes. Chemically, nNHCs are best compared to phosphines, as both classes of ligands are monodentate, two-electron donors. However, nNHCs have many properties that set them apart from phosphines. The former are generally regarded as better σ donors than the latter, while the π-acceptor strength is often thought to be weak, although the carbene carbon atom has a formally empty p_π orbital.[17] Theoretical studies showed that π-electron density is donated from the two nitrogen atoms in the 1- and 3-positions of the azole ring to the empty p_π orbital of the sp^2-hybridized carbene carbon atom.[18] The electron donation increases upon coordination of the carbene carbon atom to a metal center, partly to offset its σ donation to the metal. This diminishes the ability of the carbene to accept electron density from the metal atom, but enables it to be a good σ donor.[19] The cyclic π delocalization in unsaturated six-π-electron imidazol-2-ylidenes yields weak aromaticity in the five-membered ring, but N→C π donation in C–C saturated imidazoline-2-ylidenes is not much less than in the former species.[18b] Thus, the carbene carbon atom with its two N substituents in nNHCs can be regarded as a three-center, four-electron π system.[20]

The weakness of π backdonation from the metal to the nNHC ligand in complexes of Groups 10 and 11 has been controversially discussed in some recent work. Whereas some π interaction was suggested for bis(carbene) complexes of nickel(0) and platinum(0), the complexes of Group 11 metals were suggested to be purely σ-bonded.[21] In contrast, a significant amount of π interaction between Group 11 metals and carbene ligands was suggested on the basis of structural data and by visual inspection of the shape of the calculated molecular orbitals.[22,23] An energy-decomposition analysis of [(nNHC)TMX] and $[(nNHC)_2TM]^+$ complexes (TM = Cu, Ag, Au; X = F, Cl, Br, I) showed that π backdonation in the latter compounds is not much weaker than in classical Fischer carbene complexes that bear two π-donor groups R at the CR_2 carbene ligand.[24]

Recent computational evidence[25] shows that the bonding situation for nNHCs may be even more varied. When the metal centers are very electrophilic, they may be stabilized by π donation from the nNHC ligand to an electron-deficient metal center. A computational study by Jacobsen et al.[26] suggests that nNHCs are not exclusively σ donors, but can also receive significant π-electron density; in the case of electrophilic d^0 systems, even π donation from the nNHC is possible. Thus, nNHCs may act as π acids or π bases, depending on the metal center to which they are coordinated. The stereoelectronic parameters that are associated with NHC ligands were recently summarized in a comprehensive review by Díez-González and Nolan.[27]

It would be a significant contribution to the knowledge of the strength and the nature of metal–ligand bonding if the complexes L_nTM(nNHC), L_nTM(aNHC), and L_nTM(IMID) were calculated and the bonding situation analyzed with modern quantum-chemical methods. Herein, we report theoretical studies of early, middle, and late transition metals with the ligands nNHC, aNHC, and IMID. The calculated complexes are $[Cl_4TM(nNHC)]$ (**1TM(n)**), $[Cl_4TM(aNHC)]$ (**1TM(a)**), and $[Cl_4TM(IMID)]$ (**1TM(I)**) (TM = Ti, Zr, Hf), $[(CO)_5TM(nNHC)]$ (**2TM(n)**), $[(CO)_5TM(aNHC)]$ (**2TM(a)**), and $[(CO)_5TM(IMID)]$ (**2TM(I)**) (TM = Cr, Mo, W), $[(CO)_4TM(nNHC)]$ (**3TM(n)**), $[(CO)_4TM(aNHC)]$ (**3TM(a)**), and $[(CO)_4TM(IMID)]$ (**3TM(I)**) (TM = Fe, Ru, Os), and [ClTM(nNHC)] (**4TM(n)**), [ClTM(aNHC)] (**4TM(a)**), and [ClTM(IMID)] (**4TM(I)**) (TM = Cu, Ag, Au). The investigated complexes are shown in Table 1. The theoretically predicted equilibrium geometries and metal–ligand bond-dissociation energies (BDEs) are given. The nature of the metal–ligand interactions was investigated with energy decomposition analysis (EDA). We compared the nature of the bonding in $[(CO)_5TM(L)]$ (TM = Cr, Mo, W) for L = nNHC, aNHC, and IMID with the bonding in the related phosphine complexes $[(CO)_5TM(PX_3)]$ (X = H, Me, F, Cl), which was analyzed by us in a previous paper.[28] To the best of our knowledge, this is the first comprehensive study that compares the bonding behavior of the different tautomers of imidazole as well as phosphine in a variety of chemical environments by using a quantitative bonding analysis that goes beyond descriptions in terms of orbital interactions.[43]

Table 1. Overview of the complexes investigated.

Descriptor	Complex[a]	Central atoms
1	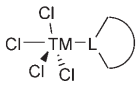	Ti (**1Ti**) Zr (**1Zr**) Hf (**1Hf**)
2	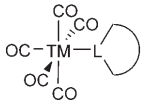	Cr (**2Cr**) Mo (**2Mo**) W (**2W**)
3	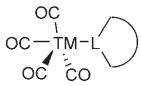	Fe (**3Fe**) Ru (**3Ru**) Os (**3Os**)
4	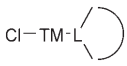	Cu (**4Cu**) Ag (**4Ag**) Au (**4Au**)

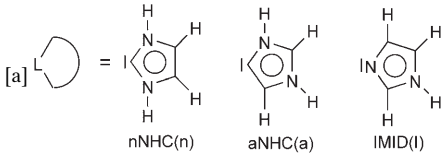

Thus, for the first time, we prove rigorously much of what was previously only speculation.

Results and Discussion

Geometries and Energies

The optimized geometries of the free imidazole isomers nNHC, aNHC, and IMID at the BP86/TZ2P level are shown in Figure 1, along with the most important bond lengths and angles and the relative energies of the compounds. The full set of geometrical data is listed in the Supporting Information, Table S1. The imidazole molecule IMID is 26.7 kcal mol^{-1} lower in energy than the nNHC isomer, which in turn is 17.4 kcal mol^{-1} more stable than the aNHC form. This is in agreement with the previous work by SEC, who reported that the relative energies are IMID (0.0 kcal mol^{-1}) < nNHC (28.9 kcal mol^{-1}) < aNHC (48.9 kcal mol^{-1}).[14a]

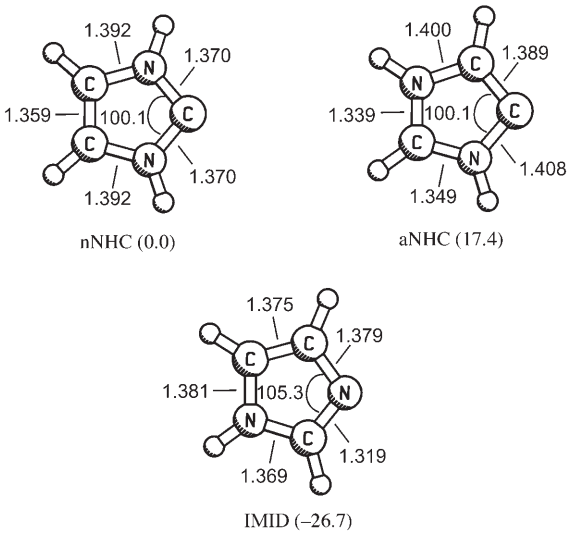

Figure 1. Calculated geometries of the ligands at the BP86/TZ2P level of theory. Relative energies (kcal mol^{-1}) are given in parentheses.

Figure 2 shows the optimized geometries of the calculated complexes [Cl_4TM(L)], [$(CO)_5$TM(L)], [$(CO)_4$TM(L)], and [ClTM(L)] (L = nNHC, aNHC, IMID). The full set of geometrical data is given in the Supporting Information, Table S2.

The equilibrium geometries of the Group 4 complexes [Cl_4TM(nNHC)] and [Cl_4TM(aNHC)] (TM = Ti, Zr, Hf) have the carbene ligand in the equatorial position, whereas the imidazole ligand IMID occupies an axial position in [Cl_4TM(IMID)] (Figure 2). The energy differences between the axial and equatorial isomers of the [Cl_4TM(L)] complexes are quite small. Geometry optimization of the axial form of [Cl_4TM(nNHC)] and [Cl_4TM(aNHC)] gave structures that, in all cases, are less than 1 kcal mol^{-1} higher in energy than the equatorial energy minima. The axial forms have one or sometimes two imaginary modes with low frequencies. Likewise, the equatorial isomers of [Cl_4TM(IMID)] are less than 1 kcal mol^{-1} less stable than the axial forms.

Table 2 gives the optimized TM–L bond lengths, the relative energies of the isomers, and the calculated TM–L BDEs. The calculated data reveal interesting trends. The aNHC ligand is always more strongly bonded than the nNHC ligand. The difference ΔD_e lies between 3.7 kcal mol^{-1} for **3FeL** and **2CrL** and 5.8 kcal mol^{-1} for **1HfL**. The stronger TM–aNHC bonds make the energy difference between the complexes TM(nNHC) and TM(aNHC) smaller than those between the free ligands, so that the TM(nNHC) complexes are only 11.7–13.7 kcal mol^{-1} lower in energy than the TM(aNHC) species. For the BDEs of the TM(nNHC) and TM(IMID) compounds, much larger differences were calculated, as the latter molecules have significantly weaker metal–ligand bonds than the former. The differences ΔD_e are between 14.2 kcal mol^{-1} for **1ZrL** and 28.4 kcal mol^{-1} for **4AuL**. The weaker bonds yield smaller energy differences between the TM(nNHC) and TM(IMID) compounds than between the free nNHC and IMID ligands, to the extent that the TM(nNHC) and TM(IMID) complexes are energetically nearly degenerate for **3TM(L)** and **4AuL**. Without exception, the trend in BDE for the three ligands with all the metals is **TM(a) > TM(n) > TM(I)**. The trend in BDE for the different groups of the transition metals of each row is **1TM(L) < 2TM(L) < 3TM(L) < 4TM(L)**, except for the Mo/Ru and W/Os species, for which the trend is **2TM(L) > 3TM(L)**. These exceptions do not arise from a reversal in the trend of the metal–ligand attraction but rather from differences in the preparation energies of the metal fragments (see below). The BDEs for all ligands in the complexes **1TM(L)** decrease in the order third row > second row > first row. For the complexes **2TM(L)** and **4TM(L)**, the D_e values exhibit the BDE trend third row > first row >

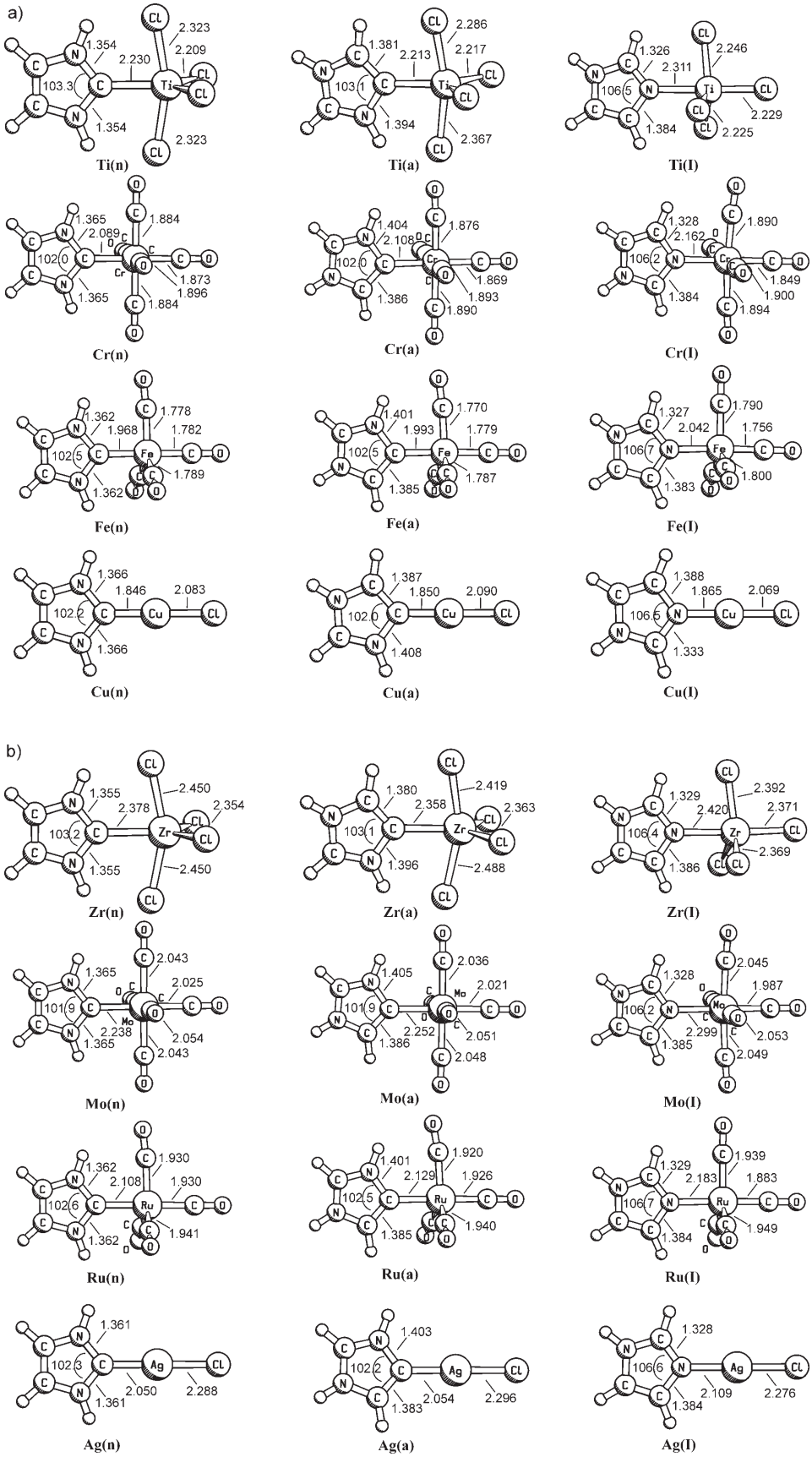

Figure 2. Geometries of all the complexes at the BP86/TZ2P level of theory. Distances are given in Å, angles in degrees.

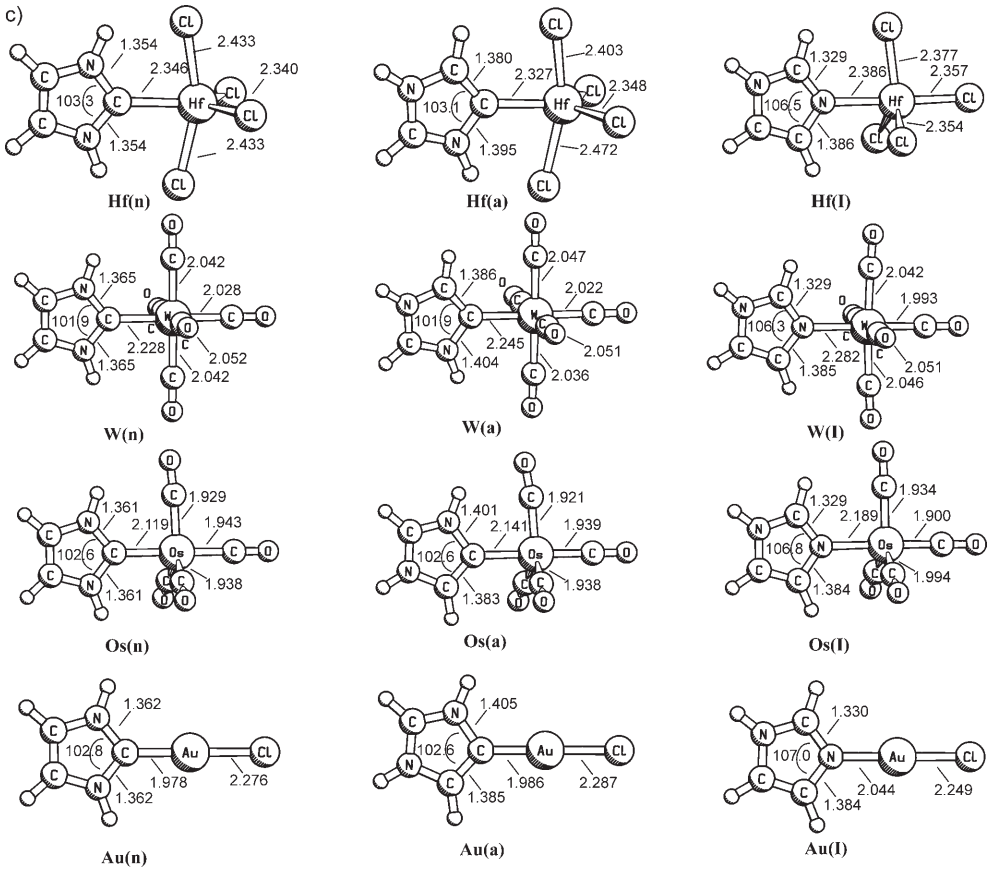

Figure 2. (Continued)

second row, whereas for **3TM(L)**, the order is first row > third row > second row.

Thus, it is clear that the significantly stronger metal–ligand bonds of the nNHC ligand relative to those of IMID largely compensate for the lower energy of the free imidazole ligand. Therefore, the complexes TM(nNHC) may become lower in energy than their TM(IMID) isomers. This was also found by SEC, who calculated 17 TM(nNHC) complexes and their TM(IMID) isomers.[14a] The energy differences between the **TM(a)** and **TM(n)** complexes are also somewhat decreased relative to the free ligands because the TM–aNHC bonds are stronger than the TM–nNHC bonds. However, as the effect is not as large as in the case of nNHC/IMID, the **TM(n)** complexes always remain lower in energy than their **TM(a)** counterparts. SEC calculated only one metal fragment, $PtCl_3^-$, bonded to the ligand aNHC.

Table 2. Metal–ligand bond lengths d(TM–L), relative energies E_{rel} of the complexes, bond-dissociation energies D_e, and free dissociation energies D_0^{298} of the ligands.[a]

L	nNHC				aNHC				IMID			
	d(TM–L)	E_{rel}	D_e	D_0^{298}	d(TM–L)	E_{rel}	D_e	D_0^{298}	d(TM–L)	E_{rel}	D_e	D_0^{298}
Free L		0.0				17.4				−26.7		
1Ti	2.230	0.0	26.5	12.0	2.213	11.9	32.0	17.4	2.311	−12.1	11.8	−1.9
1Zr	2.378	0.0	33.5	18.8	2.358	11.7	39.1	24.4	2.420	−12.6	19.3	5.7
1Hf	2.346	0.0	34.0	19.3	2.327	11.7	39.8	25.0	2.386	−12.4	19.7	6.0
2Cr	2.090	0.0	52.2	36.6	2.108	13.7	55.9	41.7	2.161	−5.5	31.0	17.2
2Mo	2.238	0.0	49.4	36.5	2.252	13.6	53.1	39.9	2.299	−8.0	30.7	17.5
2W	2.228	0.0	55.7	42.7	2.245	13.5	59.6	46.4	2.282	−6.2	35.1	22.0
3Fe	1.968	0.0	60.1	45.4	1.993	13.7	63.8	48.3	2.042	0.4	33.0	18.1
3Ru	2.108	0.0	48.0	36.0	2.129	13.4	52.0	39.3	2.183	−1.5	22.8	10.7
3Os	2.119	0.0	53.8	40.9	2.141	13.2	58.0	44.1	2.189	0.8	26.3	12.9
4Cu	1.846	0.0	67.9	56.0	1.850	13.4	71.9	59.9	1.865	−6.6	47.7	36.1
4Ag	2.050	0.0	53.4	42.0	2.054	12.8	57.9	45.9	2.109	−7.3	33.9	22.5
4Au	1.978	0.0	76.3	64.4	1.986	13.2	80.6	68.0	2.044	1.8	47.9	35.8

[a] Bond lengths in Å, energies in kcal mol^{-1}. All calculations were performed at the BP86/TZ2P level.

The $[Cl_3Pt(aNHC)]^-$ complex was found to be 23.3 kcal mol^{-1} higher in energy than the $[Cl_3Pt(nNHC)]^-$ isomer, whereas the free ligand aNHC is only 20.0 kcal mol^{-1} less stable than nNHC.[14a]

Bonding Analysis

To understand the nature of the metal–ligand bonds, we first discuss the electronic structure of the free ligands nNHC, aNHC, and IMID. Table 3 shows the five highest occupied molecular orbitals (HOMOs) and the lowest unoccupied molecular orbital (LUMO) of the molecules.

Table 3. Kohn–Sham valence orbitals (BP86/TZ2P) of the ligands nNHC, aNHC, and IMID.[a]

Orbital	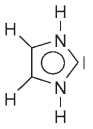	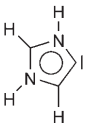	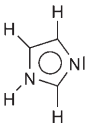
LUMO	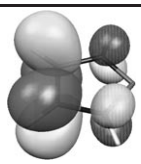 −0.32 (a_2)	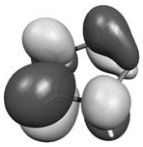 −1.25 (a″)	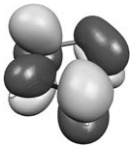 −0.57 (a″)
HOMO	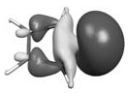 −4.97 (a_1)	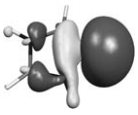 −4.25 (a′)	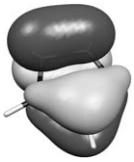 −5.76 (a″)
HOMO-1	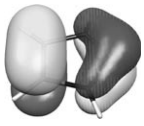 −5.85 (b_1)	 −5.49 (a″)	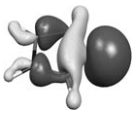 −6.33 (a′)
HOMO-2	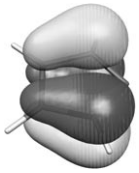 −7.50 (a_2)	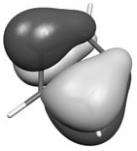 −7.76 (a″)	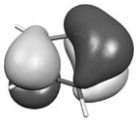 −7.03 (a″)
HOMO-3	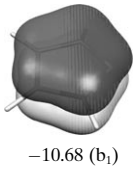 −10.68 (b_1)	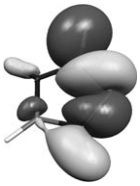 −9.79 (a′)	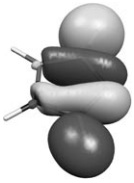 −9.99 (a′)
HOMO-4	 −10.71 (a_1)	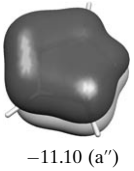 −11.10 (a″)	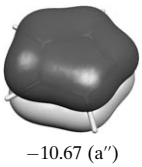 −10.67 (a″)

[a] Orbital energies are given below in eV.

The HOMOs of the heterocyclic carbenes nNHC and aNHC are the lone-pair orbitals of the σ carbon atom, which have only small coefficients at the other carbon and nitrogen atoms. Below the HOMO, each cyclic carbene has three occupied π orbitals that look very similar to the π orbitals in the cyclopentadienyl anion, Cp^-. We showed in previous work that free nNHCs have some aromatic character.[18b] The shape of the orbitals indicates that aNHC and IMID may also contain some aromatic stability. The nitrogen σ lone-pair orbital of the imidazole ligand IMID is HOMO-1. Notably, this orbital is energetically much lower lying (−6.33 eV) than the carbon σ lone-pair orbitals of nNHC (−4.97 eV) and aNHC (−4.25 eV). The energy levels of these orbitals suggest that the σ-donor strength of the ligands has the trend aNHC > nNHC > IMID.

Figure 3 shows schematically the relevant orbital interactions between a transition metal and the nNHC ligand by using C_{2v} symmetry. A similar outline applies for the other

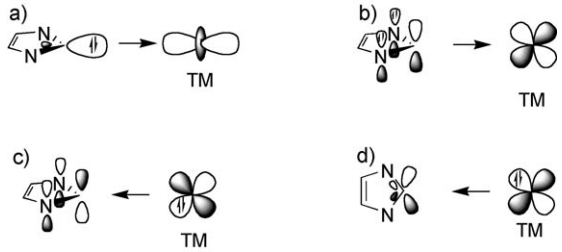

Figure 3. Schematic representation of the orbital interactions between a transition-metal fragment and the nNHC ligand by using C_{2v} symmetry. a) L→TM σ donation. b) L→TM $\pi_\perp$ donation. c) TM→L $\pi_\perp$ backdonation. d) TM→L $\pi_\parallel$ backdonation.

two ligands. Figure 3a and b displays the nNHC→TM σ and π donations, whereas Figure 3c shows the nNHC←TM π backdonation. The nNHC ligand also has a second π orbital that is in the plane of the ring. This orbital may give rise to in-plane $\pi_\parallel$ interactions with the metal. Figure 3d shows the nNHC←TM $\pi_\parallel$ backdonation. This interaction, however, is not relevant as it is only the out-of-plane $\pi_\perp$ contribution that is considered as π bonding in most discussions of carbene complexes. The in-plane $\pi_\parallel$ interactions are usually absorbed in the σ interactions. We follow this convention. EDA calculations were carried out with C_s symmetry for most molecules, which means that the a″ orbitals give the $\pi_\perp$ contribution, whereas the a′ orbitals give the $\sigma+\pi_\parallel$ interactions. For the Group 11 complexes **4TM(L)** with L = nNHC, we also report EDA calculations with C_{2v} symmetry, which make it possible to distinguish between $\pi_\perp$ and $\pi_\parallel$ interactions.

The EDA results for Group 4 d^0 metal compounds (Table 4) suggest that the nature of the Cl_4TM–L interactions is quite similar among the ligands L = nNHC, aNHC, and IMID. The percentage contribution of the orbital interactions varies between 30.8 and 34.7%, which means that the Cl_4TM–L bonds are roughly two-thirds electrostatic and

Table 4. EDA results for the Cl_4TM-L bond of the complexes **1TM(L)** at the BP86/TZ2P level.[a]

	1Ti(n)	1Zr(n)	1Hf(n)	1Ti(a)	1Zr(a)	1Hf(a)	1Ti(I)	1Zr(I)	1Hf(I)
ΔE_{int}	−55.5	−55.5	−59.0	−63.6	−64.0	−67.8	−23.6	−28.6	−30.2
ΔE_{Pauli}	115.3	109.8	125.7	120.9	116.1	133.6	65.7	62.5	72.8
ΔE_{elstat}[b]	−112.0	−111.8	−127.7	−120.5	−121.8	−139.3	−59.4	−61.5	−70.1
	(65.6)	(67.7)	(69.1)	(65.3)	(67.6)	(69.2)	(66.6)	(67.5)	(68.0)
ΔE_{orb}[b]	−58.8	−53.4	−57.0	−64.0	−58.3	−62.0	−29.9	−29.6	−32.9
	(34.4)	(32.3)	(30.9)	(34.7)	(32.4)	(30.8)	(33.4)	(32.5)	(32.0)
$\Delta E_{\sigma}(a')$[c]	−51.3	−46.2	−49.3	−55.4	−50.1	−53.3	−25.5	−24.7	−27.6
	(87.2)	(86.5)	(86.4)	(86.6)	(85.8)	(85.9)	(85.5)	(83.3)	(83.9)
$\Delta E_{\pi}(a'')$[c]	−7.6	−7.2	−7.8	−8.6	−8.3	−8.8	−4.3	−4.9	−5.3
	(12.8)	(13.5)	(13.6)	(13.4)	(14.2)	(14.1)	(14.5)	(16.7)	(16.1)
$\Delta E_{\pi}(L\rightarrow TM)$[d]	−3.8	−3.4	−3.7	−4.5	−4.0	−4.4	−1.7	−2.1	−2.4
	(48.7)	(45.0)	(45.1)	(51.6)	(47.8)	(47.8)	(39.8)	(42.3)	(43.7)
$\Delta E_{\pi}(TM\rightarrow L)$[d]	−4.0	−4.1	−4.5	−4.2	−4.4	−4.8	−2.6	−2.9	−3.1
	(51.3)	(55.0)	(54.9)	(48.4)	(52.2)	(52.2)	(60.2)	(57.7)	(56.3)
ΔE_{prep}	29.0	22.0	24.9	31.6	24.8	28.0	11.8	9.2	10.5
$\Delta E_{prep}(L)$	1.7	1.6	1.7	2.0	1.7	1.8	0.5	0.5	0.6
$\Delta E_{prep}(TM)$	27.2	20.4	23.2	29.7	23.1	26.2	11.3	8.7	9.9
$\Delta E\ (=-D_e)$	−26.5	−33.5	−34.1	−32.0	−39.1	−39.8	−11.8	−19.3	−19.7
d(TM–L)	2.230	2.378	2.346	2.213	2.358	2.327	2.311	2.420	2.386

[a] Energies in kcal mol^{-1}, bond lengths in Å. [b] The values in parentheses (%) give the percentage contribution to the total attractive interactions $\Delta E_{elstat}+\Delta E_{orb}$. [c] The values in parentheses (%) give the percentage contribution to the total orbital interactions ΔE_{orb}. [d] The values in parentheses (%) give the percentage contribution to the total nonsynergetic π-bond interactions $\Delta E_{\pi}(L\rightarrow TM)+\Delta E_{\pi}(TM\rightarrow L)$.

about one third covalent. The breakdown of the orbital term ΔE_{orb} into contributions from σ and π orbitals indicates that the orbital interactions come mainly from the σ orbitals, which contribute 83.3–87.2% to ΔE_{orb} in all cases. The trend of the total interaction energy ΔE_{int} for the three ligands neatly follows that of the σ-donation term $\Delta E_{\sigma}(a')$ and the orbital term ΔE_{orb}: aNHC > nNHC ≫ IMID (Table 4). This trend is in agreement with the energy levels of the highest occupied σ lone-pair orbitals of the ligands (the HOMOs of the cyclic carbenes and HOMO-1 of the imidazole; Table 3). Previous EDA studies of transition-metal compounds showed that ΔE_{orb} is often in agreement with the trend of the overall bond strength even when it is a minor contributor to the attractive interactions, although there are also cases in which the electrostatic interactions ΔE_{elstat} or the Pauli repulsion ΔE_{Pauli} determine the trend.[29] We will return to the correlation between the various energy terms of the EDA and the strength of the binding interactions at the end of this section.

Table 4 shows that the π-orbital contributions $\Delta E_{\pi}(a'')$ to the overall attractive interactions as well as to ΔE_{orb} in the series **1TM(L)** are rather small. However, the L→TM π donation and the TM→L π backdonation are nearly equal. The ability of the nNHC ligand to serve as a π donor was recently suggested by Nolan and co-workers[25] and by Jacobsen et al.[26] Importantly, the Cl_4TM-L interaction energies, ΔE_{int}, differ significantly from the BDE values, D_e, because the preparation energies of the Cl_4TM fragments (which have a tetrahedral equilibrium geometry) are rather large, particularly for the carbene ligands (Table 4). However, the D_e values exhibit the same trend for the three ligands as the ΔE_{int} values, that is, aNHC > nNHC ≫ IMID. Thus, it is not justified to use the D_e values as the only measure of the intrinsic strength of the metal–ligand interactions. For example, the titanium compound $[Cl_4Ti(nNHC)]$ has a smaller BDE ($D_e = 26.5$ kcal mol^{-1}) than its zirconium homologue $[Cl_4Zr(nNHC)]$ ($D_e = 33.5$ kcal mol^{-1}), although the ΔE_{int} values of these compounds are the same (−55.5 kcal mol^{-1}). The BDE values and the intrinsic interaction energies ΔE_{int} of the heaviest metal hafnium for all the ligands are slightly larger than for the lighter metals. This is in agreement with the common knowledge that transition metals of the third row generally have stronger bonds than those of the second and first rows.

Table 5 gives the EDA results for the Group 6 d^6 compounds $[(CO)_5TM(L)]$ with the labels **2TM(L)**. The BDEs of these complexes are clearly larger than those of the d^0 compounds $[Cl_4Ti(L)]$ (Table 4). This comparison is somewhat misleading, as the preparation energies of the former compounds are very small in comparison to those of the latter. In fact, the interaction energies of $[(CO)_5TM(nNHC)]$ and $[(CO)_5TM(aNHC)]$ are actually somewhat smaller than the ΔE_{int} values of $[Cl_4Ti(nNHC)]$ and $[Cl_4Ti(aNHC)]$. The overall trend in ΔE_{int} for **2TM(L)** is the same as before: aNHC > nNHC ≫ IMID, and the nature of the bonding in $[(CO)_5TM(L)]$ is very similar to that in $[Cl_4Ti(L)]$. Again, the orbital term ΔE_{orb} contributes around one third to the attractive interactions, and the σ contribution dominates. However, the percentage of the π contribution to ΔE_{orb} is slightly larger than in $[Cl_4TM(L)]$ and comes mainly from $(CO)_5TM\rightarrow L$ π backdonation.

The EDA results for the complexes $[(CO)_5TM(L)]$ (L = aNHC, nNHC, IMID) are compared with the data for $[(CO)_5TM(PR_3)]$ (R = Me, Cl) below. We showed earlier[28] that the nature of the metal–PR_3 bond in trihalophosphine complexes (R = F, Cl) is very different from that in PH_3 or PMe_3 complexes. The orbital interactions in $[(CO)_5TM(PF_3)]$ and $[(CO)_5TM(PCl_3)]$ are stronger than in $[(CO)_5TM-$

Table 5. EDA results for the $(CO)_5TM{-}L$ bonds of the complexes **2TM(L)** at the BP86/TZ2P level.[a]

	2Cr(n)	2Mo(n)	2W(n)	2Cr(a)	2Mo(a)	2W(a)	2Cr(I)	2Mo(I)	2W(I)
ΔE_{int}	−53.9	−51.5	−58.3	−57.5	−55.4	−62.1	−31.9	−31.8	−36.6
ΔE_{Pauli}	112.3	103.7	124.3	112.5	106.7	126.0	58.4	56.5	69.2
ΔE_{elstat}[b]	−110.6	−107.8	−129.1	−113.1	−112.9	−133.5	−59.6	−59.8	−72.1
	(66.5)	(69.5)	(70.7)	(66.5)	(69.6)	(70.9)	(66.0)	(67.7)	(68.1)
ΔE_{orb}[b]	−55.7	−47.4	−53.5	−57.0	−49.2	−54.7	−30.7	−28.5	−33.7
	(33.5)	(30.5)	(29.3)	(33.5)	(30.4)	(29.1)	(34.0)	(32.3)	(31.9)
$\Delta E_{\sigma}(a')$[c]	−46.0	−38.6	−43.5	−48.2	−41.1	−45.6	−25.5	−23.4	−27.7
	(82.6)	(81.5)	(81.3)	(84.6)	(83.5)	(83.4)	(82.9)	(82.1)	(82.0)
$\Delta E_{\pi}(a'')$[c]	−9.7	−8.8	−10.0	−8.8	−8.1	−9.1	−5.3	−5.1	−6.1
	(17.4)	(18.5)	(18.7)	(15.4)	(16.5)	(16.6)	(17.1)	(17.9)	(18.0)
$\Delta E_{\pi}(L\rightarrow TM)$[d]	−2.5	−2.1	−2.3	−2.8	−2.4	−2.6	−1.5	−1.5	−1.7
	(23.6)	(22.5)	(21.7)	(30.1)	(29.0)	(28.0)	(27.7)	(29.3)	(28.2)
$\Delta E_{\pi}(TM\rightarrow L)$[d]	−7.9	−7.2	−8.3	−6.5	−6.0	−6.8	−3.8	−3.6	−4.4
	(76.4)	(77.5)	(78.3)	(69.9)	(71.0)	(72.0)	(72.3)	(70.7)	(71.8)
ΔE_{prep}	2.2	2.2	2.6	1.7	2.3	2.5	1.0	1.2	1.5
$\Delta E_{prep}(L)$	0.7	0.4	0.4	0.5	0.5	0.5	0.3	0.3	0.4
$\Delta E_{prep}(TM)$	1.5	1.8	2.2	1.1	1.9	2.0	0.6	0.9	1.1
$\Delta E\ (=-D_e)$	−51.7	−49.3	−55.7	−55.9	−53.1	−59.6	−31.0	−30.6	−35.1
d(TM–L)	2.090	2.238	2.228	2.108	2.252	2.245	2.161	2.299	2.282

[a] Energies in kcal mol^{-1}, bond lengths in Å. [b] The values in parentheses (%) give the percentage contribution to the total attractive interactions $\Delta E_{elstat}+\Delta E_{orb}$. [c] The values in parentheses (%) give the percentage contribution to the total orbital interactions ΔE_{orb}. [d] The values in parentheses (%) give the percentage contribution to the total nonsynergic π-bond interactions $\Delta E_{\pi}(L\rightarrow TM)+\Delta E_{\pi}(TM\rightarrow L)$.

$(PH_3)]$ or $[(CO)_5TM(PMe_3)]$ due to more $TM\rightarrow(PR_3)$ π backdonation. However, the BDEs of the latter species are significantly larger than those of the trihalophosphine complexes. The weaker bonds in $[(CO)_5TM(PF_3)]$ and $[(CO)_5TM(PCl_3)]$ are caused by weaker electrostatic attraction due to the more pronounced s character of the phosphorus donor orbital. This leads to the orbital being more compact, which brings about less-efficient overlap with the metal nucleus. Thus, the bonding analysis of the $[(CO)_5TM(PR_3)]$ complexes reveals a striking example in which the trend of the metal–ligand interactions is not determined by the strength of the orbital interactions but by the electrostatic term.

Table 6 shows the EDA results for $[(CO)_5TM(PR_3)]$ (R = Me, Cl). A comparison with $[(CO)_5TM(L)]$ in Table 5 shows that the metal–ligand bonding is similar in both cases. As the preparation energies are always quite small, we can compare the interaction energies directly. The ΔE_{int} values of the $[(CO)_5TM(PMe_3)]$ complexes are about 10 and 15 kcal mol^{-1} smaller than those of $[(CO)_5TM(nNHC)]$ and $[(CO)_5TM(aNHC)]$, respectively. The percentage contribution of the orbital term ΔE_{orb} in the $[(CO)_5TM(PMe_3)]$ complexes is slightly higher than for the complexes of the imidazole tautomers. Interestingly, the EDA data shows that the ΔE_{π} contribution of the $[(CO)_5TM(PMe_3)]$ complexes is higher and the ΔE_{σ} contribution is lower than in the $[(CO)_5TM(L)]$ (L = aNHC, nNHC, IMID) complexes. For the trichlorophosphine complexes $[(CO)_5TM(PCl_3)]$, the ΔE_{π} contribution is, as expected, even higher. Previous studies of the electronic effects of nNHC complexes suggest that they are stronger σ donors than phosphines.[13,17e,f] This is in agreement with our EDA results. Notably, the phosphine ligands have two degenerate π components for the π-orbital interactions, which are only compared to the out-of-plane

Table 6. EDA results for the $(CO)_5TM{-}PR_3$ bonds at the BP86/TZ2P level.[a]

	$[Cr(CO)_5PMe_3]$	$[Mo(CO)_5PMe_3]$	$[W(CO)_5PMe_3]$	$[Cr(CO)_5PCl_3]$	$[Mo(CO)_5PCl_3]$	$[W(CO)_5PCl_3]$
ΔE_{int}	−43.7	−40.9	−46.4	−27.8	−26.1	−31.1
ΔE_{Pauli}	96.5	85.6	99.3	78.4	70.1	83.3
ΔE_{elstat}[b]	−85.1	−80.7	−94.9	−49.6	−45.3	−55.8
	(60.7)	(63.8)	(65.1)	(46.7)	(47.3)	(48.8)
ΔE_{orb}[b]	−55.1	−45.8	−50.8	−56.6	−51.0	−58.5
	(39.3)	(36.2)	(34.9)	(53.3)	(52.9)	(51.2)
ΔE_{σ}[c]	−41.0	−33.1	−37.3	−30.4	−26.3	−31.2
	(74.3)	(72.3)	(73.4)	(53.7)	(51.5)	(53.3)
ΔE_{π}[c]	−14.2	−12.7	−13.5	−26.2	−24.7	−27.3
	(25.7)	(27.7)	(26.6)	(46.3)	(48.5)	(46.7)
ΔE_{prep}	2.5	3.0	2.6	1.0	2.5	2.5
$\Delta E\ (=-D_e)$	−41.2	−37.9	−43.8	−26.8	−23.7	−28.6
d(TM–L)	2.390	2.553	2.553	2.300	2.457	2.459

[a] Energies in kcal mol^{-1}, bond lengths in Å. [b] The values in parentheses (%) give the percentage contribution to the total attractive interactions $\Delta E_{elstat}+\Delta E_{orb}$. [c] The values in parentheses (%) give the percentage contribution to the total orbital interactions ΔE_{orb}.

$\pi_\perp$ contribution in the cyclic ligands. As discussed earlier, the in-plane $\pi_\parallel$ interactions of the latter are incorporated in the ΔE_σ term.

Table 7 gives the EDA results for the Group 8 d^8 compounds $[(CO)_4TM(L)]$ (**3TM(L)**). The ΔE_{int} values are 10–20 kcal mol^{-1} larger than for the Group 6 compounds $[(CO)_5TM(L)]$, but the trends and composition of the metal–ligand bonds in the two sets of molecules are nearly the same. The electrostatic bonding constitutes about two thirds of the ΔE_{int} values. The percentage of π contribution to the orbital interactions in **3TM(L)** is slightly smaller than in **2TM(L)**, but also comes mainly from TM→L π backdonation. However, the trend in BDE is different from that of the other complexes: first row > third row > second row. This is caused by the rather low preparation energies for the iron complexes and not by the intrinsically strong metal–ligand bonds.

The EDA results for the Group 10 d^{10} complexes [ClTM(L)] (**4TM(L)**; Table 8) reveal insightful differences to the previous molecules. The strength of the ClTM–L interactions is similar to that of the $[(CO)_4TM(L)]$ complexes, but the former species have a clear trend in ΔE_{int} for all the ligands: third row > first row > second row. The relative amount of covalent character (% of ΔE_{orb}) of the ClTM–L

Table 7. EDA results for the $(CO)_4TM-L$ bonds of the complexes **3TM(L)** at the BP86/TZ2P level.[a]

	3Fe(n)	3Ru(n)	3Os(n)	3Fe(a)	3Ru(a)	3Os(a)	3Fe(I)	3Ru(I)	3Os(I)
ΔE_{int}	−68.4	−68.3	−76.6	−72.5	−72.7	−81.0	−40.2	−40.6	−46.7
ΔE_{Pauli}	143.9	142.4	168.5	145.0	143.9	169.6	76.2	74.9	90.8
ΔE_{elstat}[b]	−138.0	−142.8	−168.7	−139.9	−145.9	−171.5	−74.6	−75.8	−90.3
	(65.0)	(67.8)	(68.8)	(64.3)	(67.3)	(68.4)	(64.1)	(65.6)	(65.7)
ΔE_{orb}[b]	−74.3	−67.9	−76.5	−77.6	−70.8	−79.1	−41.8	−39.7	−47.3
	(35.0)	(32.2)	(31.2)	(35.7)	(32.7)	(31.6)	(35.9)	(34.4)	(34.3)
$\Delta E_\sigma(a')$[c]	−62.8	−57.7	−65.1	−67.0	−61.4	−68.8	−35.7	−34.1	−40.6
	(84.5)	(85.0)	(85.1)	(86.3)	(86.8)	(86.9)	(85.2)	(85.9)	(85.9)
$\Delta E_\pi(a'')$[c]	−11.5	−10.2	−11.4	−10.6	−9.3	−10.3	−6.2	−5.6	−6.7
	(15.5)	(15.0)	(14.9)	(13.7)	(13.2)	(13.1)	(14.8)	(14.1)	(14.1)
$\Delta E_\pi(L\rightarrow TM)$[d]	−2.7	−2.2	−2.3	−3.3	−2.7	−2.8	−1.7	−1.5	−1.8
	(21.7)	(20.2)	(19.1)	(29.2)	(27.6)	(25.7)	(26.2)	(26.8)	(25.8)
$\Delta E_\pi(TM\rightarrow L)$[d]	−9.8	−8.7	−9.8	−8.0	−7.1	−8.1	−4.7	−4.2	−5.1
	(78.3)	(79.8)	(80.9)	(70.8)	(72.4)	(74.3)	(73.8)	(73.2)	(74.2)
ΔE_{prep}	8.3	20.2	22.8	8.7	20.7	23.0	7.2	17.8	20.5
$\Delta E_{prep}(L)$	0.6	0.6	0.7	0.8	0.8	0.9	0.5	0.5	0.6
$\Delta E_{prep}(TM)$	7.6	19.6	22.1	8.0	19.9	22.2	6.7	17.3	19.8
$\Delta E\ (=-D_e)$	−60.1	−48.0	−53.8	−63.8	−52.0	−58.0	−33.0	−22.9	−26.3
d(TM–L)	1.968	2.108	2.119	1.993	2.129	2.141	2.042	2.183	2.189

[a] Energies in kcal mol^{-1}, bond lengths in Å. [b] The values in parentheses (%) give the percentage contribution to the total attractive interactions $\Delta E_{elstat}+\Delta E_{orb}$. [c] The values in parentheses (%) give the percentage contribution to the total orbital interactions ΔE_{orb}. [d] The values in parentheses (%) give the percentage contribution to the total nonsynergic π-bond interactions $\Delta E_\pi(L\rightarrow TM)+\Delta E_\pi(TM\rightarrow L)$.

Table 8. EDA results for the ClTM–L bonds of the complexes **4TM(L)** at the BP86/TZ2P level by using C_s symmetry.[a]

	4Cu(n)	4Ag(n)	4Au(n)	4Cu(a)	4Ag(a)	4Au(a)	$4Cu^I$	$4Ag^I$	$4Au^I$
ΔE_{int}	−68.6	−53.9	−77.4	−72.7	−58.5	−81.9	−48.4	−34.4	−48.6
ΔE_{Pauli}	124.4	129.6	210.4	125.7	132.0	211.4	81.9	73.1	117.7
ΔE_{elstat}[b]	−148.1	−143.0	−217.1	−153.1	−149.4	−222.3	−95.2	−79.4	−117.8
	(76.7)	(77.9)	(75.5)	(77.2)	(78.4)	(75.8)	(73.1)	(73.9)	(70.8)
ΔE_{orb}[b]	−44.9	−40.6	−70.6	−45.3	−41.1	−70.9	−35.1	−28.0	−48.5
	(23.3)	(22.1)	(24.5)	(22.8)	(21.6)	(24.2)	(26.9)	(26.1)	(29.2)
$\Delta E_\sigma(a')$[c]	−32.9	−32.8	−57.4	−34.6	−34.1	−59.1	−27.1	−23.6	−41.1
	(73.3)	(81.0)	(81.2)	(76.4)	(83.0)	(83.4)	(77.4)	(84.1)	(84.7)
$\Delta E_\pi(a'')$[c]	−12.0	−7.7	−13.3	−10.7	−7.0	−11.8	−7.9	−4.5	−7.4
	(26.7)	(19.0)	(18.8)	(23.6)	(17.0)	(16.6)	(22.6)	(15.9)	(15.3)
$\Delta E_\pi(L\rightarrow TM)$[d]	−1.2	−0.9	−1.4	−1.2	−0.9	−1.4	−0.7	−0.6	−0.9
	(9.4)	(10.8)	(10.3)	(10.2)	(12.2)	(11.2)	(8.8)	(12.1)	(11.7)
$\Delta E_\pi(TM\rightarrow L)$[d]	−11.5	−7.3	−12.5	−10.2	−6.5	−10.9	−7.4	−4.0	−6.7
	(90.6)	(89.2)	(89.7)	(89.8)	(87.8)	(88.8)	(91.2)	(87.9)	(88.3)
ΔE_{prep}	0.7	0.5	1.0	0.9	0.6	1.2	0.6	0.5	0.7
$\Delta E_{prep}(L)$	0.5	0.5	0.7	0.6	0.6	0.8	0.6	0.4	0.7
$\Delta E_{prep}(TM)$	0.2	0.0	0.3	0.3	0.0	0.4	0.1	0.0	0.0
$\Delta E\ (=-D_e)$	−67.9	−53.4	−76.4	−71.9	−57.9	−80.6	−47.7	−33.9	−47.9
d(TM–L)	1.846	2.050	1.978	1.850	2.054	1.986	1.865	2.109	2.044

[a] Energies in kcal mol^{-1}, bond lengths in Å. [b] The values in parentheses (%) give the percentage contribution to the total attractive interactions $\Delta E_{elstat}+\Delta E_{orb}$. [c] The values in parentheses (%) give the percentage contribution to the total orbital interactions ΔE_{orb}. [d] The values in parentheses (%) give the percentage contribution to the total nonsynergic π-bond interactions $\Delta E_\pi(L\rightarrow TM)+\Delta E_\pi(TM\rightarrow L)$.

bonds in **4TM(L)** is less than that of the TM–L bonds in **1TM(L)–3TM(L)**. Interestingly, though, the percentage contribution of the π bonding in **4TM(L)** is significantly higher when the case of TM = Cu is compared to those of TM = Ag or Au. This is surprising because it is often stated that the particularly strong bonds of gold compounds are partly caused by the relativistic expansion of the valence d orbitals; this should enhance Au→L π backdonation. However, the EDA results provide striking evidence that the stronger bonds of the gold compounds are not caused by stronger π bonding, but rather by the significantly larger amount of σ bonding and, particularly, the stronger electrostatic attraction, which lead to larger ΔE_{int} values for the gold compounds. The ΔE_{σ} and ΔE_{elstat} terms are related to each other as they come mainly from the interactions of the ligand σ lone-pair orbitals with the vacant orbitals of the metal ($\Delta E_{\sigma}(a')$) and with the metal nucleus (ΔE_{elstat}).

Our data indicate that the π contributions of the C and N tautomers of imidazole ligands to the metal–ligand orbital interactions are clearly smaller than the σ contributions. The largest relative contributions were found for the copper complex [ClCu(nNHC)], in which the π bonding contributes 26.7% to the orbital interactions; the π bonding consists mainly of backdonation (90.6%) with little contribution from forward donation (9.4%). However, with the orbital interactions being only a minor contributor to the metal–ligand bonding, the bulk of the interaction is due to the electrostatic attraction between the ligand lone-pair electrons and the metal nucleus. On the other hand, the properties of a molecule may be significantly influenced by a change in a particular energy term even though that term may be a minor contributor overall. Therefore, it is not justified to neglect the π interaction. As mentioned earlier, we showed in a previous study[24] that the π-bonding contribution in metal–nNHC complexes is not substantially smaller than in Fischer carbene complexes that bear two π-donor groups at the ligand.[30]

Table 9 gives the EDA results for the complexes [ClTM(nNHC)], which were calculated with C_{2v} symmetry. Data obtained under this constraint make it possible to distinguish between the σ(a_1) and the $\pi_{\parallel}(b_2)$ interactions, that is, the two components of the σ(a′) orbital interactions under C_s symmetry. The $\pi_{\parallel}(b_2)$ interactions are significantly weaker than the σ(a_1) interactions, but they are half as strong as the $\pi_{\perp}$ contribution in [ClAg(nNHC)] and [ClAu(nNHC)].

In the light of our results, we comment on the EDA results of nNHC complexes reported by Jacobson et al.[26] They, too, concluded that the π interactions make a substantial contribution to the metal–ligand interactions, but neglected the major contribution of the electrostatic term. Moreover, the authors followed an early suggestion for interpreting EDA results in which the first two terms, ΔE_{elstat} and ΔE_{Pauli}, are added to a single term, ΔE^0, which is called the "steric-energy term".[31] It was later recognized that ΔE^0 has nothing to do with the loosely defined steric interaction that is often used to explain the repulsive interactions of bulky substituents. As ΔE_{elstat} is usually attractive and ΔE_{Pauli} repulsive, the two terms often largely cancel each other. This means that the focus of the discussion of the bonding interactions rests almost exclusively on the orbital-interaction term, ΔE_{orb}. Thus, important information about the electrostatic/covalent character of the bond, given by the ratio $\Delta E_{elstat}/\Delta E_{orb}$, is lost. Furthermore, numerical values of ΔE^0 may become negative. This leads to an nonphysical description of attractive steric interactions.

Table 9. EDA results for the ClTM–nNHC bonds of the complexes **4TM(n)** at the BP86/TZ2P level by using C_{2v} symmetry.[a]

	4Cu(n)	4Ag(n)	4Au(n)
ΔE_{int}	−68.6	−53.9	−77.4
ΔE_{Pauli}	124.4	129.6	210.4
ΔE_{elstat}[b]	−148.1 (76.7)	−143.0 (77.9)	−217.1 (75.4)
ΔE_{orb}[b]	−44.9 (23.3)	−40.6 (22.1)	−70.7 (24.6)
ΔE_{σ} (a_1)[c]	−28.0 (62.3)	−29.1 (71.7)	−50.9 (72.0)
ΔE_{δ} (a_2)[c]	−0.1 (0.2)	−0.2 (0.6)	−0.3 (0.4)
$\Delta E\pi_{\perp}$ (b_1)[c]	−11.9 (26.5)	−7.5 (18.5)	−13.0 (18.4)
$\Delta E\pi_{\parallel}$ (b_2)[c]	−5.0 (11.0)	−3.8 (9.3)	−6.5 (9.2)
ΔE_{prep}	0.7	0.5	1.0
ΔE_{prep}(L)	0.5	0.5	0.7
ΔE_{prep}(TM)	0.2	0.0	0.3
ΔE ($=-D_e$)	−67.9	−53.4	−76.4
d(TM–L)	1.846	2.050	1.978

[a] Energies in kcal mol^{-1}, bond lengths in Å. [b] The values in parentheses (%) give the percentage contribution to the total attractive interactions $\Delta E_{elstat} + \Delta E_{orb}$. [c] The values in parentheses (%) give the percentage contribution to the total orbital interactions ΔE_{orb}.

After considering the bonding interactions for the four groups of metal complexes, we return to the observed correlation between the energy levels of the highest lying σ orbital of the imidazole ligands and the strength of the interaction energies, ΔE_{int}. Figure 4 shows a graph of the correlation between the orbital and interaction energies. The trend clearly suggests that an energetically higher lying σ-donor orbital of a ligand induces stronger interactions. However, the correlation lines of the different metals cross, and the slopes of the lines vary. This indicates that, for a given ligand, the magnitude of the interaction energy of the

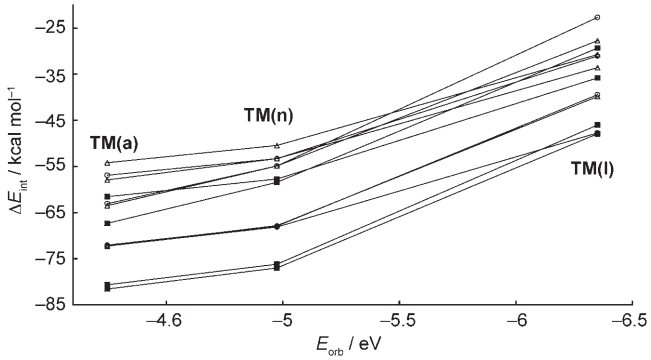

Figure 4. Correlation between the calculated interaction energy of the TM–L bonds for different metals TM and the energy level of the highest occupied σ orbital of the free ligand L. ○ = first-row, △ = second-row, ■ = third-row TM.

metal–ligand bond of a complex may not correlate with the strength of the σ-orbital interaction as the metals are varied. This is indeed the case. For example, the ΔE_{int} value for the titanium complex [Cl_4Ti(nNHC)] (−55.5 kcal mol^{-1}; Table 4) is smaller than that for the copper complex [ClCu(nNHC)] (−68.6 kcal mol^{-1}; Table 8), but the strength of the σ-orbital interaction in the latter species is much less ($\Delta E_\sigma(a') =$ −32.9 kcal mol^{-1}) than in the former ($\Delta E_\sigma(a') = -51.3$ kcal mol^{-1}). Given the rather small difference in the π-orbital contributions, we conclude that the stronger ClCu–nNHC bond relative to Cl_4Ti–nNHC is not caused by orbital interactions, but rather by the much stronger electrostatic attraction (ClCu–nNHC: −148.1 kcal mol^{-1} (Table 8); Cl_4Ti–nNHC: −112.0 kcal mol^{-1} (Table 4)). This also compensates for the stronger Pauli repulsion in the former species ($\Delta E_{Pauli} = 124.4$ kcal mol^{-1}) when compared to the latter complex ($\Delta E_{Pauli} = 115.3$ kcal mol^{-1}). This is another striking instance that complements the example of the phosphine complexes, in which the trend in bond strength is not determined by the strength of orbital interactions but by the oft-neglected electrostatic term.

To facilitate the comparison of the nature of the metal–ligand interactions between the phosphine ligands PMe_3 and PCl_3 and the NHC tautomers nNHC, aNHC, and IMID, Table 10 contains the range of the percentage contributions of ΔE_{elstat} and ΔE_{orb} to the total interaction energies ΔE_{int} as well as the σ and π contributions to the orbital interactions ΔE_{orb}. The data make it clear that the NHC tautomers are better σ-donor ligands and weaker π acceptors than the phosphine ligands, and that the metal–PR_3 interactions have a higher orbital (covalent) contribution than the metal–NHC bonds.

Conclusions

The results of this work can be summarized as follows:

- The calculations of the free tautomers nNHC, aNHC, and IMID predict that free imidazole IMID is 26.7 kcal mol^{-1} more stable than the "normal" carbene tautomer nNHC, which in turn is 17.4 kcal mol^{-1} lower in energy than the "abnormal" carbene aNHC.

- The HOMOs of the carbene species nNHC and aNHC are the carbon σ lone-pair orbitals, whereas the nitrogen σ lone-pair orbital of IMID is HOMO-1. The energy levels of the σ lone-pair orbitals suggest the trend aNHC > nNHC ≫ IMID for donor strength.

- The above trend of the σ lone-pair orbitals is in agreement with the trend in BDE for the three ligands with all metals of Groups 4, 6, 8 and 10, that is, **TM(a) > TM(n) > TM(I)**.

- The total strength of the metal–ligand bond for a given imidazole ligand depends not only on the orbital interactions but also strongly on the electrostatic attraction. Complexes **TM(L)** may have weaker orbital interactions but stronger TM−L bonds than other metals **TM′(L)** because the electrostatic attraction in TM–L is much stronger than in TM′–L.

- EDA of the TM−L bonds reveals little difference in the nature of the metal–ligand interactions of nNHC, aNHC, and IMID. The largest contribution to the attractive interactions comes from the electrostatic term, ΔE_{elstat}. The orbital term ΔE_{orb} contributes about one third to the attractive interactions in the molecules **1TM(L)**–**3TM(L)** and even less in **4TM(L)**. The contribution of the π orbitals to the metal–ligand bond is rather small for all ligands, but not negligible.

- The comparison of the EDA results for the Group 6 complexes [$(CO)_5$TM(L)] (L = nNHC, aNHC, IMID) with the phosphine complexes (L = PMe_3 and PCl_3) shows that the phosphine ligands are weaker σ donors and better π acceptors than the carbene ligands nNHC and aNHC.

Table 10. Range of the interaction energy ΔE_{int}, the percentage contributions of ΔE_{elstat} and ΔE_{orb} to the total interaction energies ΔE_{int}, and the σ and π contributions to the orbital interactions ΔE_{orb} of the metal–ligand bonds in the calculated complexes.

Ligand	$P(CH_3)_3$	PCl_3	nNHC	aNHC	IMID
ΔE_{int} [kcal mol^{-1}]	−40.9 to −46.4	−26.1 to −31.1	−51.5 to −58.3	−55.4 to −62.1	−31.8 to −36.6
ΔE_{elstat} [%]	60.7–65.1	46.7–48.8	66.5–70.7	66.5–70.9	66.0–68.1
ΔE_{orb} [%]	34.9–39.3	51.2–53.3	29.3–33.5	29.1–33.5	31.9–34.0
ΔE_σ [%]	72.3–74.3	51.5–53.7	81.3–82.6	83.4–84.6	82.0–82.9
ΔE_π [%]	25.7–27.7	46.3–48.5	17.4–18.7	15.4–16.6	17.1–18.0

Theoretical Methods

All geometries were optimized under the constraint of C_s symmetry with the ligand ring lying in the mirror plane. This enabled us to separate σ- and π-bonding contributions. These initial structures were optimized with the generalized gradient approximation (GGA) to DFT by using the exchange functional of Becke[32] in conjunction with the correlation functional of Perdew[33] (BP86). Uncontracted Slater-type orbitals (STOs) were employed as basis functions for self-consistent field (SCF) calculations.[34] The basis sets for all elements have triple-ζ quality augmented by two sets of polarization functions (Amsterdam density functional (ADF) basis set "TZ2P"). Core electrons (i.e., 1s for second- and [He]2s2p for third-period atoms including first-row transition metals, [Ne]3s3p3d for second-row, and [Ar]4s4p4d for third-row transition metals) were treated with the frozen-core approximation. This level of theory is denoted BP86/TZ2P. An auxiliary set of s, p, d, f, and g STOs was used to fit the molecular densities and to represent the Coulomb and exchange potentials accurately in each SCF cycle.[35] Scalar relativistic effects were incorporated by applying the zero-order regular approximation (ZORA).[36] Calculations were carried out with the program package ADF2006.01.[37]

Interatomic interactions were investigated by means of EDA developed independently by Morokuma[38] and by Ziegler and Rauk.[39] The bonding analysis focuses on the instantaneous interaction energy ΔE_{int} of a bond A–B between two fragments A and B in the particular electronic reference state and in the frozen geometry of AB. This interaction energy is divided into three main components [Eq. (1)]:

$$\Delta E_{int} = \Delta E_{elstat} + \Delta E_{Pauli} + \Delta E_{orb} \quad (1)$$

The term ΔE_{elstat} corresponds to the classical electrostatic interaction between the unperturbed charge distributions of the prepared atoms and is usually attractive. The Pauli repulsion, ΔE_{Pauli}, is the energy change associated with the transformation from the superposition of the unperturbed electron densities $\rho_A+\rho_B$ of the isolated fragments to the wavefunction $\Psi^0 = N\hat{A}[\Psi_A\Psi_B]$, which properly obeys the Pauli principle through explicit antisymmetrization ($\hat{A}$ operator) and renormalization (N=constant) of the product wavefunction.[37a] ΔE_{Pauli} comprises the destabilizing interactions between electrons of the same spin on either fragment. The orbital interaction ΔE_{orb} accounts for charge-transfer and polarization effects.[40] The ΔE_{orb} term can be decomposed into contributions from each irreducible representation of the point group of the interacting system. As the molecules in our study have at least C_s symmetry, it is possible to estimate quantitatively the intrinsic strength of orbital interactions from orbitals with a′ and a″ symmetry. This gives the contributions of the σ- and π-orbital interactions to the ΔE_{orb} term directly [Eq. (2)]:

$$\Delta E_{orb} = \Delta E_{\sigma}(a') + \Delta E_{\pi}(a'') \quad (2)$$

An orbital-deletion procedure recently applied by our group to the question of the strength of conjugation and hyperconjugation in molecules[41] can shed further light on the bonding interactions between the ligand and the metal. This method was also used by Jacobsen for the analysis of the transition-metal complexes of nNHCs.[26a] It is possible to split the π-interaction term $\Delta E_{\pi}(a'')$ into two terms, $\Delta E_{\pi}(L\rightarrow TM)$ and $\Delta E_{\pi}(TM\rightarrow L)$, which denote the extent of π donation from the ligand to the metal and from the metal to the ligand, respectively. This is done by repeating the EDA for all the complexes while consecutively deleting the a″ virtual orbitals of the ligand to gain information on $\Delta E_{\pi}(L\rightarrow TM)$. Repeating the same procedure for the a″ virtual orbitals of the metal provides data on $\Delta E_{\pi}(TM\rightarrow L)$. However, these terms do not add up to the $\Delta E_{\pi}(a'')$ contribution of the ΔE_{orb} term. Rather, a small residual term remains. The constraint put on the variational space causes the deletion procedure to affect all the other orbitals in the calculations so that the remaining interacting orbitals in the deletion calculations are not the same as in the undeleted ones.

To obtain the BDE, D_e (by definition with an opposite sign to that of ΔE), the preparation energy ΔE_{prep} (which gives the relaxation of the fragments into their electronic and geometrical ground states) must be added to ΔE_{int} [Eq. (3)]:

$$\Delta E\ (=-D_e) = \Delta E_{int} + \Delta E_{prep} \quad (3)$$

Further details on EDA can be found in the literature.[37]

To calculate the dissociation energies, we calculated each fragment in its optimized geometry and derived ΔE by Equation (3). All complexes and fragments investigated were characterized by an analysis of the analytically calculated harmonic frequencies as was recently implemented in ADF.[42] By applying a standard state of 298.15 K and 1 atm, thermodynamic quantities were also derived.

Acknowledgements

This work was supported by the Deutsche Forschungsgemeinschaft. Excellent service by the Hochschulrechenzentrum of the Philipps-Universität Marburg is gratefully acknowledged. Additional computer time was provided by the HLRS Stuttgart, the CSC Frankfurt, and the HHLRZ Darmstadt. G.H. thanks the National Research Foundation of South Africa (grant number SFP2005110900004) and the DAAD of Germany (grant number A/05/52686) for postdoctoral funding.

[1] K. Öfele, *J. Organomet. Chem.* **1968**, *12*, P42.
[2] H.-W. Wanzlick, H.-J. Schönherr, *Angew. Chem.* **1968**, *80*, 154; *Angew. Chem. Int. Ed. Engl.* **1968**, *7*, 141.
[3] A. J. Arduengo III, R. L. Harlow, M. Kline, *J. Am. Chem. Soc.* **1991**, *113*, 361.
[4] W. A. Herrmann, *Angew. Chem.* **2002**, *114*, 1342; *Angew. Chem. Int. Ed.* **2002**, *41*, 1290.
[5] W. A. Hermann, B. Cornils, *Angew. Chem.* **1997**, *109*, 1074; *Angew Chem. Int. Ed. Engl.* **1997**, *36*, 1048.
[6] a) A. Fürstner, *Angew. Chem.* **2000**, *112*, 3140; *Angew. Chem. Int. Ed.* **2000**, *39*, 3012; b) J. Huang, H.-J. Schanz, E. D. Stevens, S. P. Nolan, *Organometallics* **1999**, *18*, 2370; c) J. K. Huang, E. D. Stevens, S. P. Nolan, J. L. Petersen, *J. Am. Chem. Soc.* **1999**, *121*, 2674; d) M. Scholl, S. Ding, C. W. Lee, R. H. Grubbs, *Org. Lett.* **1999**, *1*, 953; e) T. Weskamp, W. C. Schattenmann, M. Spiegler, W. A. Herrmann, *Angew. Chem.* **1998**, *110*, 2631; *Angew. Chem. Int. Ed.* **1998**, *37*, 2490; f) L. Jafarpour, S. P. Nolan, *J. Organomet. Chem.* **2001**, *617*, 17.
[7] a) G. A. Grasa, M. S. Viciu, J. Huang, S. P. Nolan, *J. Org. Chem.* **2001**, *66*, 7729; b) G. A. Grasa, M. S. Viciu, J. Huang, C. Zhang, M. L. Trudell, S. P. Nolan, *Organometallics* **2002**, *21*, 2866; c) M. S. Viciu, R. F. Germaneau, S. P. Nolan, *Org. Lett.* **2002**, *4*, 4053; d) O. Navarro, R. A. Kelly, S. P. Nolan, *J. Am. Chem. Soc.* **2003**, *125*, 16194.
[8] a) A. C. Hillier, H. M. Lee, E. D. Stevens, S. P. Nolan, *Organometallics* **2001**, *20*, 4246; b) H. M. Lee, T. Jiang, E. D. Stevens, S. P. Nolan, *Organometallics* **2001**, *20*, 1255; c) L. D. Vasques-Serrano, B. T. Owens, J. M. Buriak, *Chem. Commun.* **2002**, 2518.
[9] I. E. Markò, S. Stérin, O. Buisine, G. Mignani, P. Branlard, B. Tinant, J.-P. Declerq, *Science* **2002**, *298*, 204.
[10] S. Gründemann, A. Kovacevic, M. Albrecht, J. W. Faller, R. H. Crabtree, *Chem. Commun.* **2001**, 2274.
[11] a) L. N. Appelhans, D. Zuccaccia, A. Kovacevic, A. R. Chianese, J. R. Miecznikowski, A. Macchioni, E. Clot, O. Eisenstein, R. H. Crabtree, *J. Am. Chem. Soc.* **2005**, *127*, 16299; b) S. Gründemann, A. Kovacevic, M. Albrecht, J. W. Faller, R. H. Crabtree, *J. Am. Chem. Soc.* **2002**, *124*, 10473; c) A. Kovacevic, S. Gründemann, J. R. Miecznikowski, E. Clot, O. Eisenstein, R. H. Crabtree, *Chem. Commun.* **2002**, 2580; d) A. R. Chianese, A. Kovacevic, B. M. Zeglis, K. W. Faller, R. H. Crabtree, *Organometallics* **2004**, *23*, 2461.
[12] a) X. Hu, I. Castro-Rodrigo, K. Meyer, *Organometallics* **2003**, *22*, 3016; b) X. Hu, I. Castro-Rodrigo, K. Meyer, *J. Am. Chem. Soc.* **2003**, *125*, 12237; c) H. Lebel, M. K. Janes, A. B. Charette, S. P. Nolan, *J. Am. Chem. Soc.* **2004**, *126*, 5046; d) D. Bacciu, K. J. Cavell, I. A. Fallis, L.-L. Ooi, *Angew. Chem.* **2005**, *117*, 5416; *Angew. Chem. Int. Ed.* **2005**, *44*, 5282; e) A. A. Danopoulos, N. Tsoureas, J. A. Wright, M. E. Light, *Organometallics* **2004**, *23*, 166; f) E. Kluser, A. Neels, M. Albrecht, *Chem. Commun.* **2006**, *43*, 4495; g) M. Alcarazo, S. J. Roseblade, A. R. Cowley, R. Fernandez, J. M. Brown, J. M. Lassaletta, *J. Am. Chem. Soc. 127*, 3290.
[13] R. H. Crabtree, *J. Organomet. Chem.* **2005**, *690*, 5451.
[14] a) G. Sini, O. Eisenstein, R. H. Crabtree, *Inorg. Chem.* **2002**, *41*, 602; b) A. M. Magill, B. F. Yates, *Aust. J. Chem.* **2004**, *57*, 1205.
[15] P. L. Arnold, S. Pearson, *Coord. Chem. Rev.* **2007**, *251*, 596.
[16] R. J. Sundberg, R. B. Martin, *Chem. Rev.* **1974**, *74*, 471.
[17] a) J. Schwarz, V. P. W. Böhm, M. G. Gardiner, M. Grosche, W. A. Hermann, W. Hieringer, G. Raudaschl-Sieber, *Chem. Eur. J.* **2000**, *6*, 1773; b) D. S. McGuiness, K. J. Cavell, B. W. Skelton, A. H. White, *Organometallics* **1999**, *18*, 1596; c) M. F. J. Lappert, *J. Organomet. Chem.* **1975**, *100*, 139; d) M. F. J. Lappert, *J. Chem. Soc. Dalton* **1977**, 2172; e) M. F. J. Lappert, *J. Organomet. Chem.* **1988**, *358*, 185; f) K. Öfele, W. A. Hermann, D. Mihalios, M. Elison, E. Herdtweck, W. Scherer, J. Mink, *J. Organomet. Chem.* **1993**, *459*, 177; g) L. Perrin, E. Clot, O. Eisenstein, J. Loch, R. H. Crabtree, *Inorg. Chem.* **2001**, *40*, 5806; h) T. Weskamp, F. J. Kohl, W. Hieringer, D. Gleich,

W. A. Herrmann, *Angew. Chem.* **1999**, *111*, 2573; *Angew. Chem. Int. Ed.* **1999**, *38*, 2416; i) A. T. Termaten, M. Schakel, A. W. Ehlers, M. Lutz, A. L. Spek, K. Lammertsma, *Chem. Eur. J.* **2003**, *9*, 3577; j) R. Dorta, E. D. Stevens, N. M. Scott, C. Costabile, L. Cavallo, C. D. Hoff, S. P. Nolan, *J. Am. Chem. Soc.* **2005**, *127*, 2485.

[18] a) C. Heinemann, T. Müller, Y. Apeloig, H. Schwarz, *J. Am. Chem. Soc.* **1996**, *118*, 2023; b) C. Boehme, G. Frenking, *J. Am. Chem. Soc.* **1996**, *118*, 2039.

[19] a) N. Fröhlich, U. Pidun, M. Stahl, G. Frenking, *Organometallics* **1997**, *16*, 442; b) C. Boehme, G. Frenking, *Organometallics* **1998**, *17*, 5801; c) M.-T. Lee, C.-H. Hu, *Organometallics* **2004**, *23*, 976.

[20] M. Tafipolsky, W. Scherer, K. Öfele, G. Artus, B. Pedersen, W. A. Hermann, G. S. McGrady, *J. Am. Chem. Soc.* **2002**, *124*, 5865.

[21] A. J. Arduengo, S. F. Gamper, J. C. Calabrese, F. Davidson, *J. Am. Chem. Soc.* **1994**, *116*, 4391.

[22] A. A. D. Tulloch, A. A. Danopoulos, S. Kleinhenz, M. E. Light, M. B. Hursthouse, G. Eastham, *Organometallics* **2001**, *20*, 2027.

[23] a) X. Hu, Y. Tang, P. Gantzel, K. Meyer, *Organometallics* **2003**, *22*, 612; b) X. Hu, I. Castro-Rodriguez, K. Olsen, K. Meyer, *Organometallics* **2004**, *23*, 755.

[24] D. Nemcsok, K. Wichmann, G. Frenking, *Organometallics* **2004**, *23*, 3640.

[25] N. M. Scott, R. Dorta, E. D. Stevens, A. Correa, L. Cavallo, S. P. Nolan, *J. Am. Chem. Soc.* **2005**, *127*, 3516.

[26] a) H. Jacobsen, *J. Organomet. Chem.* **2005**, *690*, 6068; b) H. Jacobsen, A. Correa, C. Costabile, L. Cavallo, *J. Organomet. Chem.* **2006**, *691*, 4350.

[27] S. Díez-González, S. P. Nolan, *Coord. Chem. Rev.* **2007**, *251*, 874.

[28] G. Frenking, K. Wichmann, N. Fröhlich, J. Grobe, W. Golla, D. Le Van, B. Krebs, M. Läge, *Organometallics* **2002**, *21*, 2921.

[29] a) G. Frenking, K. Wichmann, N. Fröhlich, C. Loschen, M. Lein, J. Frunzke, V. M. Rayón, *Coord. Chem. Rev.* **2003**, *238–239*, 55; b) M. Lein, G. Frenking in *Theory and Applications of Computational Chemistry: The First 40 Years* (Eds.: C. E. Dykstra, G. Frenking, K. S. Kim, G. E. Scuseria), Elsevier, Amsterdam, **2005**, p. 367.

[30] M. Lein, A. Szabó, A. Kovács, G. Frenking, *Faraday Discuss.* **2003**, *124*, 365.

[31] a) T. Ziegler, V. Tschinke, A. Becke, *J. Am. Chem. Soc.* **1987**, *109*, 1351; b) T. Ziegler, V. Tschinke, C. Ursenbach, *J. Am. Chem. Soc.* **1987**, *109*, 4825.

[32] A. D. Becke, *Phys. Rev. A* **1988**, *38*, 3098.

[33] a) J. P. Perdew, *Phys. Rev. B* **1986**, *33*, 8822; b) J. P. Perdew, *Phys. Rev. B* **1986**, *34*, 7406.

[34] J. G. Snijders, E. J. Baerends, P. Vernoojs, *At. Data Nucl. Data Tables* **1982**, *26*, 483.

[35] J. Krijn, E. J. Baerends, *Fit Functions in the HFS Method: Internal Report* (in Dutch), Vrije Universiteit, Amsterdam, **1984**.

[36] a) E. Van Lenthe, E. J. Baerends, J. G. Snijders, *J. Chem. Phys.* **1993**, *99*, 4597; b) E. Van Lenthe, E. J. Baerends, J. G. Snijders, *J. Chem. Phys.* **1994**, *101*, 9783; c) E. Van Lenthe, A. Ehlers, E. J. Baerends, *J. Chem. Phys.* **1999**, *110*, 8943.

[37] a) F. M. Bickelhaupt, E. J. Baerends in *Reviews In Computational Chemistry, Vol. 15* (Eds.: K. B. Lipkowitz, D. B. Boyd), Wiley-VCH, New York, **2000**, p. 1; b) G. Te Velde, F. M. Bickelhaupt, E. J. Baerends, C. Fonseca Guerra, S. J. A. Van Gisbergen, J. G. Snijders, T. Ziegler, *J. Comput. Chem.* **2001**, *22*, 931.

[38] K. Morokuma, *J. Chem. Phys.* **1971**, *55*, 1236.

[39] a) T. Ziegler, A. Rauk, *Inorg. Chem.* **1979**, *18*, 1755; b) T. Ziegler, A. Rauk, *Inorg. Chem.* **1979**, *18*, 1558.

[40] F. M. Bickelhaupt, N. M. M. Nibbering, E. M. Van Wezenbeek, E. J. Baerends, *J. Phys. Chem.* **1992**, *96*, 4864.

[41] I. Fernandez, G. Frenking, *Chem. Eur. J.* **2006**, *12*, 3617.

[42] a) A. Berces, R. M. Dickson, L. Y. Fan, H. Jacobsen, D. Swerhone, T. Ziegler, *Comput. Phys. Commun.* **1997**, *100*, 247; b) H. Jacobsen, A. Berces, D. P. Swerhone, T. Ziegler, *Comput. Phys. Commun.* **1997**, *100*, 263.

[43] An EDA of the binding of nNHC, phosphines, and other ligands in gold complexes was recently published: P. Pyykkö, N. Runeberg, *Chem. Asian J.* **2006**, *1*, 623.

Received: August 1, 2007
Published online: October 15, 2007

